

Boundary conformal field theory, holography and bulk locality

Pinaki Banerjee^a, Parijat Dey^b and Dipyendu Dhar^b

^a*Indian Institute of Technology Gandhinagar, Department of Physics, Gujarat 382355, India*

^b*Department of Astrophysics and High Energy Physics,
S.N. Bose National Centre for Basic Sciences, Salt Lake, Kolkata 700106, India*

pinaki.banerjee@iitgn.ac.in, parijat.dey@bose.res.in,
dipyendu.dhar@bose.res.in

ABSTRACT: We study bulk locality in a scalar effective field theory (EFT) in AdS background in presence of an end-of-the-world (EOW) brane. The holographic dual description is given in terms of a boundary conformal field theory (BCFT). We compute the two point correlation function of scalar operators in the BCFT using the one-loop Witten diagrams and compare its analytic structure with the constraints imposed by boundary conformal symmetry. We find that the loop-corrected correlator derived from a local bulk description is not fully compatible with BCFT expectations. This result places nontrivial constraint on bulk locality in holographic BCFT constructions and identifies BCFT correlators as sensitive probes of quantum bulk dynamics in presence of boundaries.

Contents

1	Introduction	1
2	Review of boundary conformal field theory	3
3	Bulk perspective of BCFT	5
3.1	Witten diagrams	6
3.2	Quartic vertex	8
3.3	Cubic vertex	11
4	Discussions and conclusion	12
A	Details of tadpole diagram	13
B	Details of bubble diagram	15

1 Introduction

One of the central lessons of the AdS/CFT correspondence [1] is that a higher dimensional space-time with local dynamics can emerge from a lower dimensional conformal field theory (CFT). In the large- N , strongly coupled regime, correlation functions in a d dimensional local CFT reorganize in a manner consistent with a bulk description governed by an effective field theory (EFT) on AdS_{d+1} . At long wavelengths, this EFT is local: interactions are described by local vertices, propagators have standard short-distance singularities, and correlators exhibit the analytic structure expected of a local quantum field theory in curved spacetime. This emergence of locality is highly nontrivial, given that the CFT itself is defined without reference to space-time locality in the bulk.

A crucial conceptual distinction in this context is between *coarse locality* and *sharp locality*. Coarse locality refers to the statement that bulk physics is local on scales comparable to the AdS radius and is visible already at tree level in the bulk through lower point correlators. Sharp locality is a much stronger requirement: it asserts that the bulk admits a local EFT description at parametrically short distances and that this description remains valid order by order in the $1/N$ expansion. Sharp locality is encoded not merely in the existence of a bulk Lagrangian, but in the detailed analytic structure of CFT correlators – specifically, in particular kinematic limits where the allowed singularities are fully fixed by conformal invariance.

In AdS/CFT, sharp locality was analyzed in a seminal work by Heemskerk, Penedones, Polchinski, and Sully (HPPS) [2]. They demonstrated that the consistency of the CFT four point function, together with

large- N factorization and conformal symmetry, imposes stringent constraints on the allowed analytic structure of the correlators. In particular, the controlled behavior of logarithmic terms in specific limits imply that the dual bulk theory must be local up to a finite number of derivatives at each order in perturbation theory. In this sense, HPPS showed that locality in the bulk is not an independent assumption but an emergent consequence of CFT consistency conditions.

Boundary conformal field theories (BCFTs) provide a clean and calculable setting to examine how introducing a boundary reshapes the conditions for bulk locality. The presence of a boundary reduces the symmetry group and modifies the kinematics of the correlation functions. Bulk scalar primary operators acquire non-vanishing one point functions, and the two-point function of scalar primaries depends nontrivially on a single conformal cross ratio [3–5] (see e.g. [6–18] for related works on CFTs with boundaries and defects). From the holographic point of view, BCFTs are described by AdS spacetimes terminated by an end-of-the-world (EOW) brane, as proposed in the AdS/BCFT construction [19, 20]. Boundary conditions imposed on the brane encode the BCFT data, while bulk fields propagate in a geometry that is globally distinct from pure AdS.

The BCFT two point function plays a role analogous to that of the four point function in ordinary homogeneous CFT. Its conformal block decomposition organizes contributions from bulk-channel and boundary-channel operators [5], and its logarithmic terms encode anomalous dimensions associated with bulk interactions. This makes the BCFT two point function a clean ‘observable’ for probing sharp locality in the presence of boundaries. From this perspective, one may regard BCFT two point functions as providing a lower-point, yet equally powerful, analogue of the HPPS four point function analysis.

Despite this close analogy, sharp locality in holographic BCFTs has received comparatively little systematic attention. The structure of BCFT correlators and their holographic representation have been explored from several complementary perspectives, including geodesic Witten diagram approximation [21, 22] and identifying constraints on when a BCFT admits a semiclassical bulk brane description [23]. AdS correlators at finite temperature have been studied holographically in [24]. Since boundaries modify the global structure of spacetime and constrain bulk propagation, it is far from obvious that a local bulk EFT should remain consistent once quantum corrections are included. Whether the HPPS logic extends to BCFTs, or whether new phenomena appear, is therefore an important open question.

In this work we address this question by performing an explicit test of sharp locality in holographic BCFT in d dimensions. We consider a scalar field propagating in AdS_{d+1} with a planar EOW brane and study one-loop Witten diagrams generated by cubic and quartic bulk interactions. Using the method of images to implement boundary conditions, we compute the contributions of these diagrams to the BCFT two-point function. This allows us to extract the analytic structure of the correlator and to compare it directly with the constraints imposed by the BCFT conformal block decomposition.

Our analysis reveals a nontrivial and intriguing outcome. For generic values of the operator dimension Δ_ϕ , the loop-corrected two-point function derived from a local bulk action fails to match the analytic structure required by boundary conformal symmetry under standard Dirichlet or Neumann boundary conditions. Since these constraints follow purely from BCFT kinematics, independently of any bulk

assumptions, this incompatibility demonstrates that a strictly local bulk EFT cannot consistently reproduce BCFT correlators beyond tree level. In this sense, our result provides a BCFT analogue of the HPPS locality test, but with a qualitatively different conclusion: in the presence of an EOW brane, sharp locality fails already at one-loop.

It is important to clarify the scope of this result. We do not interpret our findings as signaling a breakdown of the AdS/BCFT correspondence itself. Rather, our findings indicate that, under the assumptions of a purely local bulk effective field theory with standard boundary conditions, loop-level bulk amplitudes are not fully compatible with the analytic structure required by BCFT correlators. This suggests that additional ingredients – such as boundary-localized interactions (see e.g. [25, 26]), explicit defect degrees of freedom, or more general bulk descriptions beyond a local EFT – may be necessary to reconcile loop-level bulk dynamics with BCFT analyticity. Understanding which of these possibilities is realized, and how consistency is restored, is an important step toward a more complete understanding of holography in the presence of boundaries.

More broadly, our work highlights BCFT correlators as a powerful and underutilized probe of microscopic bulk locality. Compared to four-point functions in ordinary CFTs, BCFT two-point functions are technically simpler while retaining sensitivity to loop effects and analytic constraints. This makes them an attractive arena for exploring how global geometric features, such as boundaries and defects, modify the emergence of spacetime and locality in holographic duals.

The rest of the paper is organized as follows. In Section 2 we review some basics of the BCFT ideas. We discuss the computation of the two point scalar bulk correlators using Witten diagrams in Section 3. Then we discuss the incompatibility in analytic structure of these Witten diagrams with the BCFT correlators. We conclude in Section 4 with discussions on our results and future directions. The appendices provide details on the Witten diagram computations.

2 Review of boundary conformal field theory

In this section, we will review some basic concepts of a BCFT [3–5]. We consider a conformal field theory in d -dimensions bounded by a flat surface at $x^\perp = 0$. This is a BCFT defined in a semi-infinite space

$$x^\mu = (\vec{x}, x^\perp \geq 0) . \quad (2.1)$$

The boundary breaks translational invariance along x^\perp direction. This BCFT can have two types of operators: bulk operators $\phi(\vec{x}, x^\perp)$, living on the entire space x^μ and boundary operators $\hat{\phi}(\vec{x})$, localised on the boundary $x^\perp = 0$. The observables we are interested in are the correlation functions of local bulk operators. The presence of the boundary results in a non-vanishing one-point function of bulk scalar operators. Hence the non-trivial dynamical information of a BCFT is encoded in the two point correlator of these operators. Let us consider the correlator of two identical scalar operators ϕ with

scaling dimension Δ_ϕ . The operators satisfy the following boundary conditions

$$\begin{aligned} \text{Dirichlet : } & \phi(\vec{x}, x^\perp = 0) = 0 \text{ or} \\ \text{Neumann : } & \partial_{x^\perp} \phi(\vec{x}, x^\perp = 0) = 0. \end{aligned} \quad (2.2)$$

The correlator $\langle \phi(\vec{x}_1, x_1^\perp) \phi(\vec{x}_2, x_2^\perp) \rangle$ can be written in terms of the cross ratio ξ as follows

$$\langle \phi(\vec{x}_1, x_1^\perp) \phi(\vec{x}_2, x_2^\perp) \rangle = \frac{F(\xi)}{(4x_1^\perp x_2^\perp)^{\Delta_\phi}}, \quad (2.3)$$

where

$$\xi = \frac{(\vec{x}_1 - \vec{x}_2)^2 + (x_1^\perp - x_2^\perp)^2}{4x_1^\perp x_2^\perp}. \quad (2.4)$$

The function $F(\xi)$ admits an expansion in bulk channel as

$$F(\xi) = \xi^{-\Delta_\phi} \sum_{\Delta \geq 0} a_\Delta \xi^{\Delta/2} {}_2F_1\left(\frac{\Delta}{2}, \frac{\Delta}{2}; \Delta + 1 - \frac{d}{2}; -\xi\right), \quad (2.5)$$

$$(2.6)$$

where Δ is the scaling dimension of the bulk exchanged operator. In this setup the spinning intermediate operators do not appear in the OPE as they are not consistent with the boundary conformal symmetry. The coefficients a_Δ are known as the OPE coefficients.

We are interested in a BCFT with a small parameter ϵ , such that in an interacting theory the BCFT data can be expanded around the generalised free theory. This data receives corrections proportional to ϵ . Let us consider the bulk data that has the following expansion

$$\begin{aligned} \Delta_n &= 2\Delta_\phi + 2n + \epsilon \gamma_n + O(\epsilon^2), \\ a_\Delta &= a_n^{(0)} + \epsilon a_n^{(1)} + O(\epsilon^2), \quad n = 0, 1, 2, \dots \end{aligned} \quad (2.7)$$

In the bulk channel the correlator contains double trace operators $\phi \square^n \phi$ with scaling dimension Δ_n . Here γ_n denotes the bulk anomalous dimension of these double trace operators. The expansion of the function $F(\xi)$ then takes the following form

$$F(\xi) = F^{(0)}(\xi) + \epsilon F^{(1)}(\xi) + O(\epsilon^2). \quad (2.8)$$

We are interested in the anomalous dimensions appearing in the BCFT spectrum. The bulk anomalous dimensions can be extracted from the $\log \xi$ term of $F^{(1)}(\xi)$ as

$$F^{(1)}(\xi) = \log \xi \sum_n \xi^n \frac{1}{2} \langle a_n^{(0)} \gamma_n \rangle {}_2F_1(n + \Delta_\phi, n + \Delta_\phi; 2\Delta_\phi + 1 + 2n - \frac{d}{2}; -\xi) + \dots, \quad (2.9)$$

where the ellipsis denotes the non logarithmic terms. The bracket $\langle \rangle$ denotes sum over possible degenerate operators in the spectrum. We can now focus on the discontinuities of $F^{(1)}(\xi)$ in ξ . The discontinuity of any function $f(\xi)$ is defined as

$$\text{Disc}_\xi f(\xi) \equiv \lim_{\alpha \rightarrow 0^+} f(\xi + i\alpha) - f(\xi - i\alpha). \quad (2.10)$$

Note that in (2.9) there is a hypergeometric function with argument $-\xi$, which has a branch cut at $\xi \in (-\infty, -1)$ and is analytic elsewhere. On the other hand, the $\log \xi$ term has a branch cut at $\xi < 0$. As a consequence, the discontinuity in the range $\xi \in (-1, 0)$ originates only from the logarithms in (2.9), which is $\text{Disc}_{\xi < 0} \log \xi = 2\pi i$. Hence we have

$$\text{Disc}_{-1 < \xi < 0} F^{(1)}(\xi) = \pi i \sum_n \xi^n \langle a_n^{(0)} \gamma_n \rangle {}_2F_1(n + \Delta_\phi, n + \Delta_\phi; 2\Delta_\phi + 1 + 2n - \frac{d}{2}; -\xi). \quad (2.11)$$

We expect that such logarithmic singularities should also arise from the holographic dual correlator with bulk local interactions as we will discuss in the next section. Our goal is to match the discontinuities of the bulk channel expansion (2.11) with the ones of the Witten diagram computations.

3 Bulk perspective of BCFT

In this section we calculate the two point correlation function of a BCFT using the bulk dual living in AdS space with an end-of-the-world brane. We consider a bulk scalar field Φ with cubic and quartic interactions, propagating in AdS_{d+1} in presence of a brane extended along the radial direction. The bulk action in Poincaré patch coordinates $x^\mu = (y, x^\perp, \vec{x})$ is given by

$$S = \int_{x^\perp \geq 0} dx^\perp \int_{y \geq 0} dy \int_{\mathbb{R}^{d-1}} d^{d-1} \vec{x} \sqrt{g} \left(\frac{1}{2} \nabla_\mu \Phi \nabla^\mu \Phi + m^2 \Phi^2 + V(\Phi) \right), \quad (3.1)$$

with the following interaction potential

$$V(\Phi) = \delta_{\nu,1} (\lambda_3 \Phi^3 + \lambda_4 \Phi^4) + \delta_{\nu,-1} (\lambda_5 (\nabla \Phi)^4 + \dots). \quad (3.2)$$

The couplings are denoted by $\lambda_3, \lambda_4, \lambda_5$ and ellipsis denotes the higher derivative interactions. The $\delta_{\nu,\pm 1}$ serves a purpose that will become clear shortly. Here g is the Euclidean AdS metric given by

$$ds^2 = \frac{1}{y^2} \left(dy^2 + dx^\perp{}^2 + d\vec{x}^2 \right). \quad (3.3)$$

The bulk scalars can satisfy Dirichlet or Neumann boundary conditions¹

$$\begin{aligned} \text{Dirichlet : } & \Phi(\vec{x}, x^\perp = 0, y) = 0, \\ \text{Neumann : } & \partial_{x^\perp} \Phi(\vec{x}, x^\perp = 0, y) = 0. \end{aligned} \quad (3.4)$$

¹We impose Dirichlet or Neumann boundary conditions on the end-of-the-world brane, which ensure a well-defined variational principle.

We use $\nu = +1$ for Neumann and $\nu = -1$ for Dirichlet boundary conditions respectively. Note that the Kronecker delta's in (3.2) take care of the vertices relevant to a particular boundary condition. For example the first few simplest vertices on the brane are $\lambda_3 \Phi^3$ for Neumann and $\lambda_5 (\nabla \Phi)^4$ for Dirichlet. The BCFT is located at the boundary $y = 0$ and described by $(x^\perp \geq 0, \vec{x})$. The bulk field Φ can be thought of as dual to a scalar primary operator ϕ in a BCFT, with scaling dimension Δ_ϕ satisfying

$$\Delta_\phi(\Delta_\phi - d) = m^2. \quad (3.5)$$

Using the holographic dictionary the boundary field ϕ is defined by the limit

$$\Phi(\vec{x}, x^\perp, y) \xrightarrow{y \rightarrow 0} y^{\Delta_\phi} \phi(\vec{x}, x^\perp), \quad (3.6)$$

and satisfies the same boundary conditions induced by the bulk AdS space (2.2).

Now we ask the question: Can we use the bulk action (3.2) to compute the BCFT correlators with specific boundary conditions mentioned in Sec. 2 and show their equivalence explicitly?

3.1 Witten diagrams

In this section we compute $\langle \phi(\vec{x}_1, x_1^\perp) \phi(\vec{x}_2, x_2^\perp) \rangle$ from the bulk action (3.1) using the Witten diagrams describing these correlators. In order to calculate the Witten diagrams, it is useful to use the embedding space formalism [27, 28]. The embedding space coordinates are related to Poincaré patch coordinates as

$$\begin{aligned} P^A &= \{1, \vec{x}^2 + x^\perp{}^2, x^i, x^\perp\}, \\ X^A &= \frac{1}{y} \{1, \vec{x}^2 + x^\perp{}^2 + y^2, x^i, x^\perp\}, \end{aligned} \quad (3.7)$$

where $i = 1, 2, \dots, d-1$ and $A = 1, 2, \dots, d+2$. The $d+2$ -dimensional vectors P^A, X^A satisfy $X^2 = -1, P^2 = 0$. In embedding space coordinates the bulk-to-bulk and the bulk-to-boundary propagators in the absence of the brane read

$$\begin{aligned} G_{B\partial}(P, X) &= \frac{1}{(-2P \cdot X)^{\Delta_\phi}}, \\ G_{BB}(X_1, X_2) &= \frac{1}{(-\zeta)^{\Delta_\phi}} {}_2F_1 \left(\Delta_\phi, \Delta_\phi - \frac{d-1}{2}, 2\Delta_\phi - d + 1, -\frac{4}{\zeta} \right), \end{aligned} \quad (3.8)$$

where

$$\zeta = \frac{(X_1 - X_2)^2}{4}. \quad (3.9)$$

The propagators in (3.1) can be constructed from (3.8) via the method of images [25, 26]

$$\begin{aligned} G_{BB}^\nu(X_1, X_2) &= G_{BB}(X_1, X_2) + \nu G_{BB}(X_{1r}, X_2), \\ G_{B\partial}^\nu(P, X) &= G_{B\partial}(P, X) + \nu G_{B\partial}(P, X_r), \end{aligned} \quad (3.10)$$

where $X_r = X|_{x^\perp \rightarrow -x^\perp}$.

With these propagators, we will now compute the leading corrections to the two point correlator $\langle \phi(P_1)\phi(P_2) \rangle$ for different boundary conditions, perturbatively in the couplings in (3.2). For simplicity we use Neumann boundary conditions for Φ . This can be generalised to Dirichlet boundary conditions. The leading Witten diagrams corresponding to the Neumann boundary conditions are shown in Figure 1.

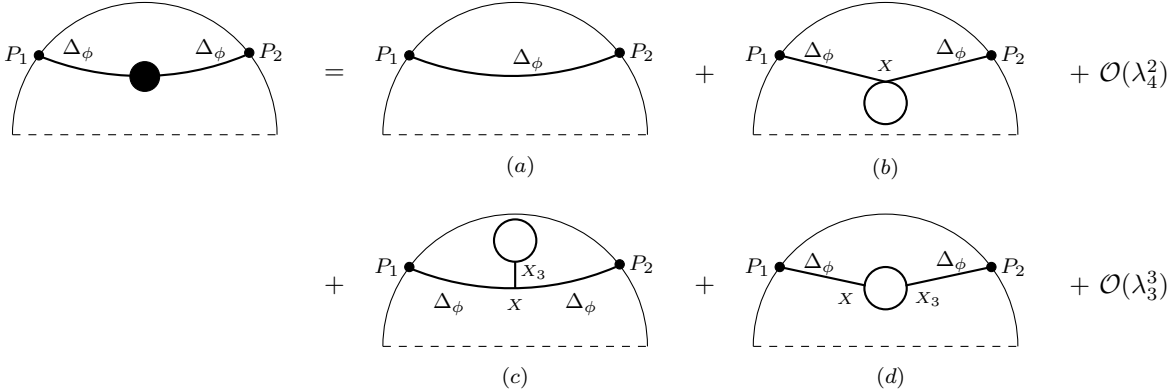


Figure 1. $\langle \phi(P_1)\phi(P_2) \rangle$ in the background (3.2) due to $\lambda_3\Phi^3 + \lambda_4\Phi^4$ interactions

To compute the Witten diagrams we use the Schwinger parameter representation of the bulk-to-boundary propagators

$$G_{B\partial}(P_i, X) = \frac{y^{\Delta_\phi}}{\Gamma(\Delta_\phi)} \int_0^\infty ds_i s_i^{\Delta_\phi-1} e^{-s_i(y^2 + (x_i^\perp - x^\perp)^2 + (\vec{x}_i - \vec{x})^2)}, \quad (3.11)$$

where

$$-2P_i \cdot X = \frac{1}{y} \left(y^2 + (x_i^\perp - x^\perp)^2 + (\vec{x}_i - \vec{x})^2 \right). \quad (3.12)$$

We also use the Mellin-Barnes representation of the Gaussian hypergeometric function for the bulk-to-bulk propagator

$$G_{BB}(X_1, X_2) = \frac{(-1)^{\Delta_\phi} \Gamma(2\Delta_\phi - d + 1)}{\Gamma(\Delta_\phi) \Gamma(\Delta_\phi - \frac{d-1}{2})} \int_{s_0-i\infty}^{s_0+i\infty} \frac{ds}{2\pi i} \frac{\Gamma(s) \Gamma(\Delta_\phi - s) \Gamma(\Delta_\phi - \frac{d-1}{2} - s)}{\Gamma(2\Delta_\phi - d + 1 - s)} 4^{-s} \zeta^{s - \Delta_\phi}, \quad (3.13)$$

where ζ is defined in (3.9).

The integration contour is located at $0 < s_0 < \min(\text{Re } a, \text{Re } b)$ i.e. $0 < s_0 < \Delta_\phi - \frac{d-1}{2}$. Note that in Figure 1 there are bulk-to-bulk propagators between coincident points. This implies a divergence coming from $G_{BB}(X_1, X)$ as $X_1 \rightarrow X$. We assume such terms can be renormalised and we set these terms to zero. Hence we have

$$\lim_{X_1 \rightarrow X} G_{BB}^\nu(X_1, X) = \nu G_{BB}(X_r, X) . \quad (3.14)$$

We now have all the necessary ingredients to compute the Witten diagrams. In the following subsections we evaluate the Witten diagrams in Figure 1 due to $\lambda_3 \Phi^3$ and $\lambda_4 \Phi^4$ and compare it with the BCFT correlator (2.8). Specifically we want to focus on the corrections of the correlator related to the bulk anomalous dimensions of the BCFT data (2.9) in what follows. We assume that any local theory in the bulk can be derived from a local Lagrangian in the weak coupling expansion in λ_3 and λ_4 . Our goal is to see if the structure of the BCFT correlator is compatible with the correlator derived from the bulk Lagrangian (3.1).

3.2 Quartic vertex

Let us now compute the leading correction to $\langle \phi(P_1) \phi(P_2) \rangle$ due to $\lambda_4 \Phi^4$ interaction in (3.1). The one-loop Witten diagram is given by the diagram depicted in Figure 1(b)

$$\begin{aligned} \langle \phi(P_1) \phi(P_2) \rangle \Big|_{\lambda_4} &= \int dX \sqrt{g} G_{B\partial}^\nu(P_1, X) G_{B\partial}^\nu(P_2, X) G_{BB}^\nu(X, X) , \\ &= \int dX \sqrt{g} \left(G_{B\partial}(P_1, X) G_{B\partial}(P_2, X) + G_{B\partial}(P_1, X_r) G_{B\partial}(P_2, X) \right. \\ &\quad \left. + G_{B\partial}(P_1, X) G_{B\partial}(P_2, X_r) + G_{B\partial}(P_1, X_r) G_{B\partial}(P_2, X_r) \right) G_{BB}(X_r, X) . \end{aligned} \quad (3.15)$$

Here we have used (3.10) to get the second line of (3.15). The volume form is given by $\sqrt{g} = y^{-d-1}$. The integrals can be computed using the tools discussed in [29]. Note that (3.15) contains four terms. We sketch below the details to evaluate the first term. The other terms can be evaluated using similar methods. Let us consider the term

$$\mathcal{C} = \int dX \sqrt{g} G_{B\partial}(P_1, X) G_{B\partial}(P_2, X) G_{BB}(X_r, X) . \quad (3.16)$$

We use (3.11) and (3.13) to rewrite the integral as

$$\begin{aligned} \mathcal{C} &= \mathcal{C}_0 \int_0^\infty dx^\perp \int_{\mathbb{R}^{d-1}} d^{d-1}x \int_0^\infty dy y^{4\Delta_\phi - 2s - d - 1} \prod_{i=1}^2 \left(\int_0^\infty ds_i s_i^{\Delta_\phi - 1} e^{-s_i(y^2 + (x_i^\perp - x^\perp)^2 + (\vec{x}_i - \vec{x})^2)} \right) \\ &\quad \times \int_{s_0 - i\infty}^{s_0 + i\infty} \frac{ds}{2\pi i} \frac{\Gamma(s)\Gamma(\Delta_\phi - s)\Gamma(\Delta_\phi - \frac{d-1}{2} - s)}{\Gamma(2\Delta_\phi - d + 1 - s)} 4^{-s} x^\perp 2^{(s - \Delta_\phi)} , \end{aligned} \quad (3.17)$$

where

$$\mathcal{C}_0 = \frac{(-1)^{\Delta_\phi} \Gamma(2\Delta_\phi - d + 1)}{\Gamma^3(\Delta_\phi) \Gamma(\Delta_\phi - \frac{d-1}{2})} . \quad (3.18)$$

We first swap the contour integrals with the bulk coordinate integrals. Then we do the integrals over the bulk coordinates y, \vec{x} and x^\perp one by one. The y and \vec{x} integrals are straightforward to evaluate. We quote below the results of these integrals

$$\int_0^\infty dy y^{4\Delta_\phi - 2s - d - 1} e^{-(s_1 + s_2)y^2} = \frac{1}{2}(s_1 + s_2)^{s + \frac{d}{2} - 2\Delta_\phi} \Gamma\left(-\frac{d}{2} + 2\Delta_\phi - s\right), \quad (3.19)$$

$$\int_{\mathbb{R}^{d-1}} d^{d-1} \vec{x} e^{-s_1(\vec{x}_1 - \vec{x})^2 - s_2(\vec{x}_2 - \vec{x})^2} = \left(\frac{\pi}{s_1 + s_2}\right)^{\frac{d-1}{2}} e^{-\frac{s_1 s_2}{s_1 + s_2}(\vec{x}_1 - \vec{x}_2)^2}. \quad (3.20)$$

The x^\perp integral can be evaluated as follows. We first use the Mellin representation of e^{-z}

$$e^{-z} = \int_{-i\infty}^{i\infty} \frac{d\tau}{2\pi i} \Gamma(\tau) z^{-\tau}, \quad (3.21)$$

and rearrange the exponential as

$$\begin{aligned} & e^{-\frac{s_1 s_2}{s_1 + s_2}(\vec{x}_1 - \vec{x}_2)^2} e^{-s_1(x_1^\perp - x^\perp)^2} e^{-s_2(x_2^\perp - x^\perp)^2} \\ &= e^{-\frac{s_1 s_2}{s_1 + s_2}(4x_1^\perp x_2^\perp \xi)} \int_{-i\infty}^{i\infty} \frac{d\tau}{2\pi i} \Gamma(\tau) (s_1 + s_2)^{-\tau} \left(x^\perp - \frac{s_1 x_1^\perp + s_2 x_2^\perp}{s_1 + s_2}\right)^{-2\tau}. \end{aligned} \quad (3.22)$$

This allows us to do the x^\perp integral resulting in the following expression

$$\begin{aligned} & \int_0^\infty dx^\perp x^{\perp 2(s - \Delta_\phi)} \left(x^\perp - \frac{s_1 x_1^\perp + s_2 x_2^\perp}{s_1 + s_2}\right)^{-2\tau} \\ &= (-1)^{1-2s+2\Delta_\phi-2\tau} \frac{\Gamma(1+2s-2\Delta_\phi)\Gamma(2\Delta_\phi+2\tau-2s-1)}{\Gamma(2\tau)} \left(\frac{s_1 + s_2}{s_1 x_1^\perp + s_2 x_2^\perp}\right)^{2\Delta_\phi+2\tau-2s-1}. \end{aligned} \quad (3.23)$$

Now we are left with the s_1, s_2, s, τ integrals. The s_1, s_2 integrals can be done by introducing a new variable ρ such that

$$1 = \int_0^\infty d\rho \delta(\rho - s_1 - s_2). \quad (3.24)$$

At this level we rescale $s_i \rightarrow \rho s_i, i = 1, 2$ and use the following identity

$$\delta(\rho - \rho s_1 - \rho s_2) = \frac{1}{\rho} \delta(1 - s_1 - s_2). \quad (3.25)$$

Note that the delta function $\delta(1 - s_1 - s_2)$ restricts the integration region of s_1, s_2 to $[0, 1]$. The ρ integral can be done first and then the s_1, s_2 -integrals using the Feynman parameterization formula

$$\frac{1}{A_1^{\alpha_1} A_2^{\alpha_2}} = \frac{\Gamma(\alpha_1 + \alpha_2)}{\Gamma(\alpha_1)\Gamma(\alpha_2)} \int_0^1 \int_0^1 ds_1 ds_2 s_1^{\alpha_1-1} s_2^{\alpha_2-1} \frac{\delta(1 - s_1 - s_2)}{(s_1 A_1 + s_2 A_2)^{\alpha_1 + \alpha_2}}. \quad (3.26)$$

We are left with the following

$$\begin{aligned} \mathcal{C} &= \mathcal{C}_0 \frac{(-1)^{1+2\Delta_\phi} \pi^{\frac{d}{2}}}{2(x_1^\perp x_2^\perp)^{\Delta_\phi}} \int_{s_0-i\infty}^{s_0+i\infty} \frac{ds}{2\pi i} \frac{(-1)^{-2s} \Gamma(s) \Gamma(\Delta_\phi - s) \Gamma(\Delta_\phi - \frac{d-1}{2} - s)}{2^{4s} \Gamma(2\Delta_\phi - d + 1 - s)} \Gamma(1 + 2s - 2\Delta_\phi) \\ &\quad \times \Gamma\left(2\Delta_\phi - s - \frac{d}{2}\right) \int_{-i\infty}^{i\infty} \frac{d\tau}{2\pi i} (-1)^{-2\tau} \xi^{\tau-s-\frac{1}{2}} \frac{\Gamma(s - \tau + \frac{1}{2}) \Gamma^2(\Delta_\phi + \tau - s - \frac{1}{2})}{\Gamma(\tau + \frac{1}{2})}. \end{aligned} \quad (3.27)$$

The τ integral results in

$$\int_{-i\infty}^{i\infty} \frac{d\tau}{2\pi i} (-1)^{-2\tau} \xi^{\tau-s-\frac{1}{2}} \frac{\Gamma(s - \tau + \frac{1}{2}) \Gamma^2(\Delta_\phi + \tau - s - \frac{1}{2})}{\Gamma(\tau + \frac{1}{2})} = \frac{\Gamma^2(\Delta_\phi)}{\Gamma(s+1)} {}_2F_1(\Delta_\phi, \Delta_\phi; s+1; -\xi). \quad (3.28)$$

Hence we have

$$\begin{aligned} \mathcal{C} &= \mathcal{C}_0 \frac{(-1)^{1+2\Delta_\phi} \pi^{\frac{d}{2}} \Gamma^2(\Delta_\phi)}{2(x_1^\perp x_2^\perp)^{\Delta_\phi}} \int_{s_0-i\infty}^{s_0+i\infty} \frac{ds}{2\pi i} \frac{(-1)^{-2s}}{2^{4s}} \frac{\Gamma(1 + 2s - 2\Delta_\phi) \Gamma(s) \Gamma(\Delta_\phi - s) \Gamma(\Delta_\phi - \frac{d-1}{2} - s)}{\Gamma(s+1) \Gamma(2\Delta_\phi - d + 1 - s)} \\ &\quad \times \Gamma\left(2\Delta_\phi - s - \frac{d}{2}\right) {}_2F_1(\Delta_\phi, \Delta_\phi; s+1; -\xi). \end{aligned} \quad (3.29)$$

We evaluate the remaining terms of (3.15) using similar techniques. Finally, collecting all the terms we have

$$\langle \phi(P_1) \phi(P_2) \rangle \Big|_{\lambda_4} = \mathcal{D}_0 \int_{s_0-i\infty}^{s_0+i\infty} \frac{ds}{2\pi i} \mathcal{A}(s) \left([1 - (-1)^{2s-2\Delta_\phi}] \mathcal{F}_s(\xi) + 2(-1)^{4s-3\Delta_\phi} \mathcal{F}_s(-1-\xi) \right), \quad (3.30)$$

where

$$\begin{aligned} \mathcal{D}_0 &= \frac{(-1)^{3\Delta_\phi-1}}{(x_1^\perp x_2^\perp)^{\Delta_\phi}} \frac{\Gamma(\Delta_\phi + 1 - \frac{d}{2})}{2^{d-2\Delta_\phi+1} \pi^{\frac{1-d}{2}} \Gamma(\Delta_\phi)}, \\ \mathcal{A}(s) &= (-1)^{-2s} \frac{\Gamma(\Delta_\phi - s) \Gamma(\Delta_\phi - s - \frac{d-1}{2})}{2^{4s} s \Gamma(1 - d - s + 2\Delta_\phi)} \Gamma(1 + 2s - 2\Delta_\phi) \Gamma(2\Delta_\phi - s - \frac{d}{2}), \\ \mathcal{F}_s(\xi) &= {}_2F_1(\Delta_\phi, \Delta_\phi; s+1; -\xi). \end{aligned} \quad (3.31)$$

Now we evaluate the s -integral in (3.30) using residue theorem by closing the s -contour to the left s -plane. This will have the following contributions from the poles in (3.31) at

(i) $s = \frac{1}{2}(2\Delta_\phi - r - 1)$, $r \in \mathbb{Z}_{\geq 0}$ from $\Gamma(1 + 2s - 2\Delta_\phi)$.

(ii) simple pole at $s = 0$.

This results in the following

$$\begin{aligned}
& \langle \phi(P_1) \phi(P_2) \rangle \Big|_{\lambda_4} \\
&= \mathcal{D}_0 \frac{\sqrt{\pi} e^{-3i\pi\Delta_\phi} \Gamma(1 - 2\Delta_\phi) \Gamma(\Delta_\phi) \Gamma(2\Delta_\phi - \frac{d}{2})}{2^{2\Delta_\phi - d} \Gamma(1 + \Delta_\phi - \frac{d}{2})} \left([(-1)^{3\Delta_\phi} - e^{i\pi\Delta_\phi}] \mathcal{F}_0(\xi) + 2\mathcal{F}_0(-1 - \xi) \right) \\
&+ \mathcal{D}_0 \sum_{r=0}^{\infty} \frac{\sqrt{\pi} (-1)^{r-2\Delta_\phi} \Gamma(\frac{1}{2}(-d+r+2)) \Gamma(\frac{1}{2}(-d+r+1) + \Delta_\phi)}{2^{4\Delta_\phi - r - 2} (-2\Delta_\phi + r + 1) \Gamma(\frac{r}{2} + 1) \Gamma(-d + \frac{r+3}{2} + \Delta_\phi)} \\
&\times \left([1 + (-1)^r] \mathcal{F}_{\Delta_\phi - \frac{r+1}{2}}(\xi) + 2e^{i\pi(\Delta_\phi + r)} \mathcal{F}_{\Delta_\phi - \frac{r+1}{2}}(-1 - \xi) \right). \tag{3.33}
\end{aligned}$$

This completes the evaluation of the diagram Figure 1(b). One can read-off the coefficients of $\log \xi$ from (3.33) which, in turn, provides us with the information of the anomalous dimensions of the bulk operators in the BCFT as mentioned in (2.9). However, expanding (3.33) around $\xi \sim 0$ does not give any $\log \xi$ term, but only power law terms in ξ .

At this level we can futher use (2.10) to calculate the discontinuity of (3.33). Note that the Witten diagram contains two hypergeometric functions with arguments $-\xi$ and $1 + \xi$, which have branch cuts at $\xi \in (-\infty, -1)$ and $\xi \in (0, \infty)$ respectively. As a result, the discontinuity of (3.33) in the range $\xi \in (-1, 0)$ vanishes. Matching the discontinuity of (3.33) with (2.11) we get

$$\langle a_n^{(0)} \gamma_n \rangle = 0, \forall n. \tag{3.34}$$

The statement (3.34) suggests a mismatch in the analytic struture of the correlator obtained via Witten diagrams and BCFT. This incompatibility indicates that a purely local quartic bulk interaction is insufficient to reproduce BCFT correlator at loop level under standard boundary conditions.

It is therefore natural to investigate whether one-loop diagrams generated by cubic bulk interactions can alter this conclusion, and in particular whether their contributions can restore the analytic structure required by boundary conformal symmetry. This possibility is analyzed in the subsequent subsection.

3.3 Cubic vertex

In this section we calculate the leading correction of $\langle \phi(P_1) \phi(P_2) \rangle$ due to cubic interaction $\lambda_3 \Phi^3$ in (3.1). The leading correction comes from the Witten diagrams at $O(\lambda_3^2)$ as depicted in (c) and (d) of Figure 1. These are the tadpole and bubble diagrams which can be evaluated by the following

$$\langle \phi(P_1) \phi(P_2) \rangle \Big|_{\lambda_3^2} = \mathcal{I}_{tad} + \mathcal{I}_{bub},$$

$$\text{where } \mathcal{I}_{tad} = \int dX_3 \sqrt{g} \int dX \sqrt{g} G_{B\partial}^\nu(P_1, X) G_{B\partial}^\nu(P_2, X) G_{BB}^\nu(X, X_3) G_{BB}^\nu(X_3, X_3), \tag{3.35}$$

$$\mathcal{I}_{bub} = \int dX_3 \sqrt{g} \int dX \sqrt{g} G_{B\partial}^\nu(P_1, X) G_{B\partial}^\nu(P_2, X_3) G_{BB}^\nu(X, X_3)^2. \tag{3.36}$$

These integrals can be evaluated using the methods described in the previous subsection. The details can be found in the appendices [A](#) and [B](#). It turns out that there are no contribution coming from the bubble diagram. Taking into account the contributions from the tadpole diagram we get the following

$$\begin{aligned} & \langle \phi(P_1) \phi(P_2) \rangle \Big|_{\lambda_3^2} \\ &= \mathcal{P}_0 \int \frac{ds}{2\pi i} \int \frac{ds_4}{2\pi i} \int \frac{d\alpha}{2\pi i} \int \frac{d\tau_1}{2\pi i} \mathcal{B}(s, \tau_1, \alpha, s_4) \\ & \times \left([(-1)^{-2s+2\Delta_\phi+2\tau_1} - (-1)^{2s-2\Delta_\phi-2\tau_1}] \mathcal{F}_{s-\tau_1+\frac{1}{2}}(\xi) + 2(-1)^{1+6s-5\Delta_\phi-6\tau_1} \mathcal{F}_{s-\tau_1+\frac{1}{2}}(-1-\xi) \right), \end{aligned} \quad (3.37)$$

where

$$\mathcal{P}_0 = \frac{(-1)^{2\Delta_\phi}}{(x_1^\perp x_2^\perp)^{\Delta_\phi}} \frac{\Gamma^2(\Delta_\phi + 1 - \frac{d}{2})}{2^{2d-6\Delta_\phi} \pi^{\frac{1}{2}-d} \Gamma^2(\Delta_\phi)}, \quad (3.38)$$

$$\begin{aligned} \mathcal{B}(s, \tau_1, \alpha, s_4) &= \frac{(-1)^{d+s_4-2\alpha-3\Delta_\phi} \Gamma(s_4) \Gamma(\Delta_\phi - s) \Gamma(\Delta_\phi - \frac{d-1}{2} - s) \Gamma(\Delta_\phi - \frac{d-1}{2} - s_4)}{2^{4s+2\alpha+4s_4} \Gamma(2\Delta_\phi - d + 1 - s) \Gamma(2\Delta_\phi - d + 1 - s_4) \Gamma(\alpha + \frac{1}{2}) \Gamma(\tau_1 + \frac{1}{2}) \Gamma(\frac{3}{2} + s - \tau_1)} \\ & \times \Gamma(d + s_4 + 2\alpha - 3\Delta_\phi) \Gamma(-d - s_4 + 3\Delta_\phi) \Gamma(-d - s - s_4 - \alpha + 3\Delta_\phi) \\ & \times \Gamma(1 + 2s - 2\Delta_\phi) \Gamma(-1 - 2s + 2\Delta_\phi + 2\tau_1) \Gamma(2 + 2s - 2\Delta_\phi - 2\tau_1) \\ & \times \Gamma\left(\frac{1-d}{2} + s - s_4 - \alpha + \Delta_\phi - \tau_1\right) \Gamma\left(\frac{d-1}{2} + s_4 + \alpha - \Delta_\phi + \tau_1\right). \end{aligned} \quad (3.39)$$

Here also we find that the Witten diagram contains contributions from two hypergeometric functions with arguments $-\xi$ and $1 + \xi$, which have branch cuts at $\xi \in (-\infty, -1)$ and $\xi \in (0, \infty)$ respectively. Hence the cubic diagrams can also not reproduce the analytic structure of the BCFT correlator (2.11).

To summarise our findings, for generic values of Δ_ϕ , the bulk interactions in (3.2) could not generate the terms at one-loop in the two point correlator of the BCFT which we expect from (2.9). We have demonstrated this for Neumann boundary conditions. This also holds for Dirichlet boundary condition with quartic interaction vertex.

4 Discussions and conclusion

We have shown that the one-loop correction to the BCFT two-point correlator obtained from a local bulk effective action in AdS with an end-of-the-world brane is not compatible with the analytic structure required by boundary conformal symmetry under standard boundary conditions. This incompatibility cannot be removed by local counter terms or field redefinitions and therefore places a sharp constraint on the validity of a strictly local bulk description.

Our results show that maintaining consistency at loop level requires additional ingredients beyond a local bulk effective field theory with standard boundary conditions. Possible resolutions include brane-localized interactions, explicit defect degrees of freedom, modified boundary conditions, or intrinsically nonlocal bulk dynamics. More broadly, this work establishes BCFT two-point functions as precise

probes of microscopic bulk locality and provides a concrete framework for exploring how boundaries and defects modify the emergence of spacetime in holographic duals.

There are several natural extensions of the present analysis. It would be interesting to understand whether the observed breakdown of sharp bulk locality persists for fields with spin, in particular for gauge fields and gravitons, where boundary conditions are more constrained by symmetry. Another important direction is to investigate whether the incompatibility can be resolved by introducing explicit boundary degrees of freedom or brane-localized interactions (see e.g. [25, 26]), and how such modifications are encoded in BCFT data. Extending the analysis to higher-loop corrections, other geometries with defects, or to time-dependent and Lorentzian setups may further clarify the interplay between boundaries, quantum corrections and bulk locality. It would also be interesting to include dynamical gravity and examine whether gravitational backreaction or induced gravitational dynamics on the brane modify the loop-level analytic structure of BCFT correlators. Moreover, semiclassical and geodesic approximations to the relevant Witten diagrams may provide useful geometric insight into the origin of the non-analytic structures and help connect exact loop results with an effective spacetime picture of bulk propagation. Finally, it would be valuable to develop a systematic criterion – analogous to the HPPS analysis in standard AdS/CFT – for characterizing when holographic theories with boundaries admit a sharply local bulk description. We hope to investigate some of these intriguing possibilities in future work.

Acknowledgments

We thank Apratim Kaviraj and Alok Laddha for useful discussions. PB would like to acknowledge the support provided by Anusandhan National Research Foundation (ANRF), India through the Ramanujan fellowship grant RJF/2023/000007. PD is supported by ANRF Early Career Research Grant ANRF/ECRG/2024/000247/PMS. PD thanks the Yukawa Institute for Theoretical Physics at Kyoto University, where this work was completed during “Progress of Theoretical Bootstrap”.

A Details of tadpole diagram

In this section we discuss the details of evaluating the integral in (3.35). There are total eight terms in the integrand. We discuss below the procedure to evaluate one of these terms. The other terms can be evaluated using similar techniques. Let us evaluate the following term for $\nu = 1$

$$\mathcal{I}_{tad}^{(1)} = \int dX_3 \sqrt{g} \int dX \sqrt{g} G_{B\partial}(P_1, X) G_{B\partial}(P_2, X) G_{BB}(X, X_3) G_{BB}(X_{3r}, X_3). \quad (\text{A.1})$$

Using 3.13 we write

$$G_{BB}(X, X_3) = (-1)^{\Delta_\phi} \frac{\Gamma(c)}{\Gamma(a)\Gamma(b)} \int_{s_0-i\infty}^{s_0+i\infty} \frac{ds_4}{2\pi i} \frac{\Gamma(s_4)\Gamma(a-s_4)\Gamma(b-s_4)}{\Gamma(c-s_4)} 4^{-s_4} \zeta_1^{s_4-\Delta_\phi}, \quad (\text{A.2})$$

with

$$\zeta_1 = \frac{-2 - 2X_3 \cdot X}{4} = \frac{\bar{\zeta}}{4y y_3}, \quad (\text{A.3})$$

and

$$\bar{\zeta} = (y - y_3)^2 + (x^\perp - x_3^\perp)^2 + (\vec{x} - \vec{x}_3)^2. \quad (\text{A.4})$$

The a, b, c 's are defined as

$$a = \Delta_\phi, \quad b = \Delta_\phi - \frac{d-1}{2}, \quad c = 2\Delta_\phi - d + 1. \quad (\text{A.5})$$

Next we write $\bar{\zeta}^{s_4 - \Delta_\phi}$ in terms of Schwinger parameter

$$\bar{\zeta}^{s_4 - \Delta_\phi} = \frac{1}{\Gamma(\Delta_\phi - s_4)} \int_0^\infty ds_5 s_5^{\Delta_\phi - s_4 - 1} e^{-s_5((y - y_3)^2 + (x^\perp - x_3^\perp)^2 + (\vec{x} - \vec{x}_3)^2)}. \quad (\text{A.6})$$

Putting these together we write (A.1) as

$$\mathcal{I}_{tad}^{(1)} = \int_0^\infty ds_5 s_5^{\Delta_\phi - s_4 - 1} \int \frac{ds}{2\pi i} \frac{ds_4}{2\pi i} \frac{\Gamma(s)\Gamma(a-s)\Gamma(b-s)\Gamma(s_4)\Gamma(b-s_4)}{4^{s+2s_4-\Delta_\phi}\Gamma(c-s)\Gamma(c-s_4)} \left(\prod_{i=1}^2 \int_0^\infty ds_i s_i^{\Delta_\phi - 1} \right) \mathcal{I}_{tot}, \quad (\text{A.7})$$

where

$$\begin{aligned} \mathcal{I}_{tot} = & \int dy dx^\perp d^{d-1}\vec{x} dy_3 dx_3^\perp d^{d-1}\vec{x}_3 (x_3^\perp)^{2s-2\Delta_\phi} y^{3\Delta_\phi - d - 1 - s_4} y_3^{3\Delta_\phi - d - 1 - s_4 - 2s} \\ & \times e^{-s_5((y - y_3)^2 + (x^\perp - x_3^\perp)^2 + (\vec{x} - \vec{x}_3)^2)} e^{-s_1(y^2 + (x_1^\perp - x^\perp)^2 + (\vec{x}_1 - \vec{x})^2)} e^{-s_2(y^2 + (x_2^\perp - x^\perp)^2 + (\vec{x}_2 - \vec{x})^2)}. \end{aligned} \quad (\text{A.8})$$

We perform the integrals over the bulk coordinates $y, x^\perp, \vec{x}, y_3, x_3^\perp, \vec{x}_3$ in (A.8). First we do the y, y_3 integrals by rewriting the exponentials as

$$e^{-s_5(y - y_3)^2} e^{-s_1 y^2} e^{-s_2 y^2} = e^{-(s_1 + s_2 + s_5) \left(y - \frac{s_5 y_3}{s_1 + s_2 + s_5} \right)^2} e^{-y_3^2 \frac{s_5(s_1 + s_2)}{s_1 + s_2 + s_5}}. \quad (\text{A.9})$$

Then using the integral representation (3.21) we write

$$e^{-(s_1 + s_2 + s_5) \left(y - \frac{s_5 y_3}{s_1 + s_2 + s_5} \right)^2} = \int_{-i\infty}^{i\infty} \frac{d\alpha}{2\pi i} \Gamma(\alpha) (s_1 + s_2 + s_5)^{-\alpha} \left(y - \frac{s_5 y_3}{s_1 + s_2 + s_5} \right)^{-2\alpha}. \quad (\text{A.10})$$

Now we do the y and y_3 integrals which results in

$$\begin{aligned} & \int_0^\infty dy \int_0^\infty dy_3 y^{-d-1+3\Delta_\phi-s_4} y_3^{3\Delta_\phi-2s-d-1-s_4} e^{-s_5(y - y_3)^2 - s_1 y^2 - s_2 y^2} \\ & = \int_{-i\infty}^{i\infty} \frac{d\alpha}{2\pi i} (-1)^{-2\alpha+d-3\Delta_\phi+s_4} \Gamma(-d - s_4 + 3\Delta_\phi) \Gamma(d + 2\alpha + s_4 - 3\Delta_\phi) \Gamma(-d - s - \alpha - s_4 + 3\Delta_\phi) \\ & \times \frac{\Gamma(\alpha)}{2\Gamma(2\alpha)} (s_1 + s_2 + s_5)^{-s} s_5^{-\alpha+s} (s_1 + s_2)^{\alpha+d-3\Delta_\phi+s+s_4}. \end{aligned} \quad (\text{A.11})$$

Next we do the \vec{x}, \vec{x}_3 integrals

$$\int_{\mathbb{R}^{d-1}} d^{d-1}\vec{x} d^{d-1}\vec{x}_3 e^{-s_5(\vec{x} - \vec{x}_3)^2} e^{-s_1(\vec{x}_1 - \vec{x})^2} e^{-s_2(\vec{x}_2 - \vec{x})^2} = \pi^{d-1} (s_5(s_1 + s_2))^{\frac{1-d}{2}} e^{-\frac{s_1 s_2}{s_1 + s_2}(\vec{x}_1 - \vec{x}_2)^2}. \quad (\text{A.12})$$

Finally we do the x^\perp, x_3^\perp integrals using (3.21) twice. This results in

$$\begin{aligned}
& \int_0^\infty dx^\perp dx_3^\perp x_3^{\perp 2s-2\Delta_\phi} e^{-s_5(x^\perp-x_3^\perp)^2-s_1(x_1^\perp-x^\perp)^2-s_2(x_2^\perp-x^\perp)^2} \\
&= \int_{-i\infty}^{i\infty} \frac{d\tau_1}{2\pi i} \frac{d\tau_2}{2\pi i} (-1)^{1-2\tau_2} \Gamma(\tau_1) \Gamma(\tau_2) s_5^{-\tau_1} \frac{\Gamma(2\tau_1 + 2\Delta_\phi - 2s - 1)}{\Gamma(2\tau_1) \Gamma(2\tau_2)} \Gamma(2s - 2\Delta_\phi + 1) \Gamma(2 + 2s - 2\Delta_\phi - 2\tau_1) \\
&\times (s_1 x_1^\perp + s_2 x_2^\perp)^{2(-\tau_1 - \tau_2 + s + 1 - \Delta_\phi)} (s_1 + s_2)^{2\tau_1 + \tau_2 + 2(\Delta_\phi - s - 1)} e^{-\frac{s_1 s_2}{s_1 + s_2} (x_1^\perp - x_2^\perp)^2} \Gamma(2(\tau_1 + \tau_2 + \Delta_\phi - s - 1)). \tag{A.13}
\end{aligned}$$

We have now evaluated the bulk integrals. Next we evaluate the s_1, s_2, s_5 integrals. In order to evaluate those integrals we introduce two variables ρ and λ such that

$$1 = \int_0^\infty d\lambda \delta(\lambda - s_1 - s_2 - s_5) \int_0^\infty d\rho \delta(\rho - s_1 - s_2), \tag{A.14}$$

and insert it in the integral. Then we rescale $s_i \rightarrow \rho s_i, i = 1, 2, 5$ and $\lambda \rightarrow \lambda\rho$ and do the integrals over $\rho, \lambda, s_5, s_2, s_1$ and τ_2 . This results in the following

$$\mathcal{I}_{tad}^{(1)} = -\mathcal{P}_0 \int \frac{ds}{2\pi i} \frac{ds_4}{2\pi i} \frac{d\alpha}{2\pi i} \frac{d\tau_1}{2\pi i} \mathcal{B}(s, s_4, \alpha, \tau_1) \mathcal{F}_{s+\frac{1}{2}-\tau_1}(\xi). \tag{A.15}$$

where $\mathcal{F}_s(\xi), \mathcal{P}_0, \mathcal{B}(s, s_4, \alpha, \tau_1)$ are defined in (3.32), (3.38) and (3.39) respectively.

Finally, evaluating all the terms in (3.35) we obtain (3.37).

B Details of bubble diagram

In this appendix, we give the details of evaluating the bubble diagram (3.36). This diagram contains contribution from total eight terms. We describe below how to evaluate one of those. The other diagrams can be evaluated in a similar fashion. Let us focus on the following term

$$\mathcal{I}_{bub}^{(1)} = \int dX \sqrt{g} \int dX_3 \sqrt{g} G_{B\partial}(P_1, X) G_{B\partial}(P_2, X_{3r}) G_{BB}(X_3, X_r)^2. \tag{B.1}$$

We use the Mellin-Barnes representation for the bulk-bulk propagator

$$\begin{aligned}
G_{BB}^2(X_3, X_r) &= \frac{(-1)^{2\Delta_\phi}}{(2\pi i)^2} \frac{\Gamma^2(c)}{\Gamma^2(a) \Gamma^2(b)} \int ds \int ds_3 \frac{\Gamma(s) \Gamma(s_3) \Gamma(a-s) \Gamma(a-s_3) \Gamma(b-s) \Gamma(b-s_3)}{\Gamma(c-s) \Gamma(c-s_3)} \\
&\times 4^{-s-s_3} \zeta^{s+s_3-2\Delta_\phi} \tag{B.2}
\end{aligned}$$

where

$$\zeta = \frac{\bar{\zeta}}{4yy_3}, \quad \bar{\zeta} = (y - y_3)^2 + (\vec{x} - \vec{x}_3)^2 + (x^\perp + x_{3\perp})^2. \tag{B.3}$$

We use the Schwinger parameterisation for

$$\bar{\zeta}^{s+s_3-2\Delta_\phi} = \frac{1}{\Gamma(2\Delta_\phi - s - s_3)} \int_0^\infty ds_5 s_5^{2\Delta_\phi - s - s_3 - 1} e^{-s_5((y-y_3)^2 + (\vec{x}-\vec{x}_3)^2 + (x^\perp + x_{3\perp})^2)}. \tag{B.4}$$

We write the bulk-boundary propagators as described in (3.11). Let us first do the coordinate integrals

$$\begin{aligned} \mathcal{I}_c &= \int dX dX_3 \frac{(yy_3)^{\Delta_\phi}}{(yy_3)^{s+s_3-2\Delta_\phi+d+1}} e^{-s_1(y^2+(\vec{x}-\vec{x}_1)^2+(x^\perp-x_1^\perp)^2)} e^{-s_2(y_3^2+(\vec{x}_2-\vec{x}_3)^2+(x_2^\perp+x_3^\perp)^2)} \\ &\quad \times e^{-s_5((y-y_3)^2+(\vec{x}-\vec{x}_3)^2+(x^\perp+x_3^\perp)^2)} \\ &= \mathcal{I}_y \mathcal{I}_v \mathcal{I}_x, \end{aligned} \quad (\text{B.5})$$

where $\mathcal{I}_y, \mathcal{I}_v, \mathcal{I}_x$ refer to the y, \vec{x}, x^\perp integrals and are defined below. The y, y_3 integrals result in

$$\begin{aligned} \mathcal{I}_y &= \int_0^\infty dy dy_3 (yy_3)^{3\Delta_\phi-s-s_3-d-1} e^{-s_1 y^2 - s_2 y_3^2 - s_5(y-y_3)^2} \\ &= \int d\tau \frac{4^{-\tau}(-1)^{d+s+s_3-3\Delta_\phi-2\tau} \sqrt{\pi}}{\Gamma(\tau+1/2)} \Gamma(3\Delta_\phi - s - s_3 - d) \Gamma(d + s + s_3 - 3\Delta_\phi + 2\tau) \\ &\quad \times \Gamma(3\Delta_\phi - \tau - d - s - s_3) s_5^{3\Delta_\phi-2\tau-d-s-s_3} (s_1 s_2 + s_1 s_5 + s_2 s_5)^{d+s+s_3-3\Delta_\phi+\tau}. \end{aligned} \quad (\text{B.6})$$

The \vec{x}, \vec{x}_3 integrations result in

$$\mathcal{I}_v = \int d^{d-1}\vec{x} d^{d-1}\vec{x}_3 e^{-s_1(\vec{x}-\vec{x}_1)^2} e^{-s_2(\vec{x}_2-\vec{x}_3)^2} e^{-s_5(\vec{x}-\vec{x}_3)^2} = \frac{\pi^{d-1}}{(s_2 s_1 + s_2 s_5 + s_1 s_5)^{\frac{d-1}{2}}} e^{-\frac{\tilde{s}s_2}{\tilde{s}+s_2}(\vec{x}_1-\vec{x}_2)^2}, \quad (\text{B.7})$$

where $\tilde{s} = \frac{s_1 s_5}{s_1 + s_5}$. Finally we are left with the x^\perp and x_3^\perp integrations

$$\mathcal{I}_x = \int dx^\perp \int dx_3^\perp e^{-s_1(x_1^\perp-x^\perp)^2 - s_2(x_2^\perp+x_3^\perp)^2 - s_5(x^\perp+x_3^\perp)^2}. \quad (\text{B.8})$$

The x^\perp integral gives

$$\begin{aligned} &\int_0^\infty dx^\perp e^{-(s_1+s_5)\left(x^\perp + \frac{s_5 x_3^\perp - s_1 x_1^\perp}{s_1+s_5}\right)^2} e^{-\tilde{s}(x_1^\perp+x_3^\perp)^2} \\ &= \int d\tau_1 \Gamma(\tau_1) (s_1 + s_5)^{-\tau_1} \left(\frac{s_5 x_3^\perp - s_1 x_1^\perp}{s_1 + s_5}\right)^{1-2\tau_1} \frac{1}{2\tau_1 - 1} e^{-\tilde{s}(x_1^\perp+x_3^\perp)^2}. \end{aligned} \quad (\text{B.9})$$

Now we use MB representation to do the x_3^\perp integral,

$$(s_5 x_3^\perp - s_1 x_1^\perp)^{1-2\tau_1} = \int d\sigma (s_5 x_3^\perp)^\sigma (-s_1 x_1^\perp)^{1-2\tau_1-\sigma} \frac{\Gamma(-\sigma) \Gamma(2\tau_1 - 1 + \sigma)}{\Gamma(2\tau_1 - 1)}. \quad (\text{B.10})$$

Now we do the x_3^\perp integration

$$\begin{aligned} &\int_0^\infty dx_3^\perp x_3^\perp \sigma e^{-(\tilde{s}+s_2)(x_3^\perp + \frac{\tilde{s} x_1^\perp + s_2 x_2^\perp}{\tilde{s}+s_2})^2} e^{-\frac{\tilde{s}s_2}{\tilde{s}+s_2}(x_1^\perp-x_2^\perp)^2} \\ &= \int d\tau_2 \Gamma(\tau_2) (\tilde{s} + s_2)^{-1-\sigma+\tau_2} (s_2 x_2^\perp + \tilde{s} x_1^\perp)^{\sigma-2\tau_2+1} \frac{\Gamma(\sigma+1) \Gamma(-\sigma+2\tau_2-1)}{\Gamma(2\tau_2)} e^{-\frac{\tilde{s}s_2}{\tilde{s}+s_2}(x_1^\perp-x_2^\perp)^2}. \end{aligned} \quad (\text{B.11})$$

After integrating x^\perp and x_3^\perp we are left with

$$\begin{aligned} \mathcal{I}_x = & \int d\tau_1 \int d\sigma \int d\tau_2 \Gamma(\tau_1) (s_1 + s_5)^{\tau_1-1} \frac{\Gamma(\sigma+1)\Gamma(-\sigma+2\tau_2-1)}{\Gamma(2\tau_1)\Gamma(2\tau_2)} \Gamma(-\sigma)\Gamma(2\tau_1-1+\sigma)\Gamma(\tau_2) \\ & \times s_5^\sigma (-s_1 x_1^\perp)^{1-2\tau_1-\sigma} (\tilde{s} + s_2)^{-1-\sigma+\tau_2} (s_2 x_2^\perp + \tilde{s} x_1^\perp)^{\sigma-2\tau_2+1} e^{-\frac{\tilde{s}s_2}{\tilde{s}+s_2}(x_1^\perp - x_2^\perp)^2}. \end{aligned} \quad (\text{B.12})$$

Now we perform σ integration,

$$\begin{aligned} \mathcal{I}_x = & \int d\tau_1 \int d\tau_2 (-1)^{-2\tau_1} \Gamma(\tau_1) (s_1 + s_5)^{\tau_1-1} (s_1 x_1^\perp)^{2-2\tau_1} (s_2 + \tilde{s})^{\tau_2} (s_2 x_2^\perp + \tilde{s} x_1^\perp)^{-2\tau_2} \\ & \times \frac{\Gamma(\tau_2)}{s_5 (2\tau_1-1)(-2+2\tau_1+2\tau_2)} {}_2F_1 \left(1, 2\tau_2; 2\tau_1+2\tau_2-1; \frac{s_1 \tilde{s} x_1^\perp + s_1 s_2 x_1^\perp}{s_2 s_5 x_2^\perp + s_5 \tilde{s} x_1^\perp} + 1 \right) e^{-\frac{\tilde{s}s_2}{\tilde{s}+s_2}(x_1^\perp - x_2^\perp)^2}. \end{aligned} \quad (\text{B.13})$$

So we have

$$\mathcal{I}_{bub}^{(1)} = \mathcal{C}' \int ds ds_1 ds_2 ds_3 ds_5 d\tau_1 d\tau_2 (-1)^{-2\tau_1} \mathcal{M}(s, s_1, s_2, s_3, s_5, \tau_1, \tau_2) e^{-\frac{\tilde{s}s_2}{\tilde{s}+s_2}(4x_1^\perp x_2^\perp \xi)} \quad (\text{B.14})$$

where

$$\begin{aligned} \mathcal{M}(s, s_1, s_2, s_3, s_5, \tau_1, \tau_2) = & \frac{4^{-s-s_3} \Gamma(s) \Gamma(s_3) \Gamma(a-s) \Gamma(a-s_3) \Gamma(b-s) \Gamma(b-s_3) \Gamma(\tau_1) \Gamma(\tau_2)}{(x_1^\perp)^{2\tau_1-2} (2\tau_1-1) (-2+2\tau_1+2\tau_2) \Gamma(c-s) \Gamma(c-s_3) \Gamma(2\Delta_\phi - s - s_3)} \mathcal{I}_y \\ & \times \frac{s_1^{\Delta_\phi+1-2\tau_1} s_2^{\Delta_\phi-1} s_5^{2\Delta_\phi-s-s_3-2} (s_1 + s_5)^{\tau_1-1} (s_2 + \tilde{s})^{\tau_2}}{(s_1 s_2 + s_1 s_5 + s_2 s_5)^{\frac{d-1}{2}} (s_2 x_2^\perp + \tilde{s} x_1^\perp)^{2\tau_2}} {}_2F_1 \left(1, 2\tau_2, 2\tau_1+2\tau_2-1; \frac{s_1 \tilde{s} x_1^\perp + s_1 s_2 x_1^\perp}{s_5 s_2 x_2^\perp + s_5 \tilde{s} x_1^\perp} + 1 \right), \\ \mathcal{C}' = & \frac{(-1)^{2\Delta_\phi} \pi^{d-1}}{(2\pi i)^2} \frac{\Gamma^2(c)}{\Gamma^4(a) \Gamma^2(b)}. \end{aligned} \quad (\text{B.15})$$

Collecting the terms proportional to $e^{-\frac{\tilde{s}s_2}{\tilde{s}+s_2}(4x_1^\perp x_2^\perp \xi)}$ in (3.36) we get the following

$$\begin{aligned} \mathcal{I}_{bub}^\xi = & \mathcal{C}' \int ds ds_1 ds_2 ds_3 ds_5 d\tau_1 d\tau_2 \left((-1)^{-2\tau_1} + (-1)^{1-2\tau_1-2\tau_2} + (-1)^{-2\tau_2} - 1 \right) \mathcal{M}(s, s_1, s_2, s_3, s_5, \tau_1, \tau_2) \\ & \times e^{-\frac{\tilde{s}s_2}{\tilde{s}+s_2}(4x_1^\perp x_2^\perp \xi)}. \end{aligned} \quad (\text{B.16})$$

Now we evaluate the integral over τ_1 and τ_2 using the residue theorem. We have the following poles from τ_1

- (i) simple pole at $\tau_1 = \frac{1}{2}$,
- (ii) simple pole at $\tau_1 = 1 - \tau_2$,
- (iii) pole at $\tau_1 = -n_1$ where $n_1 \in \mathbb{Z}_{\geq 0}$ from $\Gamma(\tau_1)$.

Subsequently, we collect the poles in τ_2 . After evaluating the corresponding residues, the expression in (B.16) vanishes. The other terms in (3.36) can be evaluated using similar methods. It turns out that all the terms vanish after evaluating the integrals.

References

- [1] J. M. Maldacena, *The Large N limit of superconformal field theories and supergravity*, *Adv. Theor. Math. Phys.* **2** (1998) 231–252, [[hep-th/9711200](#)].
- [2] I. Heemskerk, J. Penedones, J. Polchinski and J. Sully, *Holography from conformal field theory*, *Journal of High Energy Physics* **2009** (Oct., 2009) 079–079.
- [3] D. M. McAvity and H. Osborn, *Conformal field theories near a boundary in general dimensions*, *Nucl. Phys. B* **455** (1995) 522–576, [[cond-mat/9505127](#)].
- [4] J. Cardy, *Boundary Conformal Field Theory*, *Encycl. Math. Phys.* (2006) 333–340, [[hep-th/0411189](#)].
- [5] P. Liendo, L. Rastelli and B. C. van Rees, *The Bootstrap Program for Boundary CFT_d*, *JHEP* **07** (2013) 113, [[1210.4258](#)].
- [6] F. Glorioso, P. Liendo, M. Meineri and A. Rago, *Boundary and Interface CFTs from the Conformal Bootstrap*, *JHEP* **05** (2015) 036, [[1502.07217](#)].
- [7] M. Billò, V. Gonçalves, E. Lauria and M. Meineri, *Defects in conformal field theory*, *JHEP* **04** (2016) 091, [[1601.02883](#)].
- [8] C. P. Herzog and K.-W. Huang, *Boundary Conformal Field Theory and a Boundary Central Charge*, *JHEP* **10** (2017) 189, [[1707.06224](#)].
- [9] N. Andrei et al., *Boundary and Defect CFT: Open Problems and Applications*, *J. Phys. A* **53** (2020) 453002, [[1810.05697](#)].
- [10] A. Bissi, T. Hansen and A. Söderberg, *Analytic Bootstrap for Boundary CFT*, *JHEP* **01** (2019) 010, [[1808.08155](#)].
- [11] M. Lemos, P. Liendo, M. Meineri and S. Sarkar, *Universality at large transverse spin in defect CFT*, *JHEP* **09** (2018) 091, [[1712.08185](#)].
- [12] P. Dey, T. Hansen and M. Shpot, *Operator expansions, layer susceptibility and two-point functions in BCFT*, *JHEP* **12** (2020) 051, [[2006.11253](#)].
- [13] P. Dey and A. Söderberg, *On analytic bootstrap for interface and boundary CFT*, *JHEP* **07** (2021) 013, [[2012.11344](#)].
- [14] S. Giombi and H. Khanchandani, *CFT in AdS and boundary RG flows*, *JHEP* **11** (2020) 118, [[2007.04955](#)].
- [15] E. Lauria, P. Liendo, B. C. Van Rees and X. Zhao, *Line and surface defects for the free scalar field*, *JHEP* **01** (2021) 060, [[2005.02413](#)].
- [16] L. Bianchi and D. Bonomi, *Conformal dispersion relations for defects and boundaries*, *SciPost Phys.* **15** (2023) 055, [[2205.09775](#)].
- [17] J. Chen and X. Zhou, *Aspects of higher-point functions in BCFT_d*, *JHEP* **09** (2023) 204, [[2304.11799](#)].
- [18] S. Giombi and Z. Sun, *Higher loops in AdS: applications to boundary CFT*, *JHEP* **12** (2025) 011, [[2506.14699](#)].
- [19] T. Takayanagi, *Holographic Dual of BCFT*, *Phys. Rev. Lett.* **107** (2011) 101602, [[1105.5165](#)].
- [20] M. Fujita, T. Takayanagi and E. Tonni, *Aspects of AdS/BCFT*, *JHEP* **11** (2011) 043, [[1108.5152](#)].
- [21] A. Karch and Y. Sato, *Boundary Holographic Witten Diagrams*, *JHEP* **09** (2017) 121, [[1708.01328](#)].

- [22] J. Kastikainen and S. Shashi, *Structure of holographic BCFT correlators from geodesics*, *Phys. Rev. D* **105** (2022) 046007, [[2109.00079](#)].
- [23] W. Reeves, M. Rozali, P. Simidzija, J. Sully, C. Waddell and D. Wakeham, *Looking for (and not finding) a bulk brane*, *JHEP* **12** (2021) 002, [[2108.10345](#)].
- [24] L. F. Alday, M. Kologlu and A. Zhiboedov, *Holographic correlators at finite temperature*, *JHEP* **06** (2021) 082, [[2009.10062](#)].
- [25] A. Kaviraj and M. F. Paulos, *The Functional Bootstrap for Boundary CFT*, *JHEP* **04** (2020) 135, [[1812.04034](#)].
- [26] D. Mazáč, L. Rastelli and X. Zhou, *An analytic approach to BCFT_d*, *JHEP* **12** (2019) 004, [[1812.09314](#)].
- [27] S. Weinberg, *Six-dimensional Methods for Four-dimensional Conformal Field Theories II: Irreducible Fields*, *Phys. Rev. D* **86** (2012) 085013, [[1209.4659](#)].
- [28] J. Penedones, *High Energy Scattering in the AdS/CFT Correspondence*, [0712.0802](#).
- [29] L. Rastelli and X. Zhou, *The Mellin Formalism for Boundary CFT_d*, *JHEP* **10** (2017) 146, [[1705.05362](#)].